Advanced Powder Technology 26 (2015) 644–649

Contents lists available at ScienceDirect

Advanced Powder Technology

journal homepage: www.elsevier.com/locate/apt

Original Research Paper

Low temperature hydrothermal synthesis, characterization and optical properties of strontium pyroniobate

Shahin Khademinia, Mahdi Behzad *

Department of Chemistry, Semnan University, Semnan 35351-19111, Iran

ARTICLE INFO

Article history:
Received 15 October 2014
Received in revised form 31 December 2014
Accepted 27 January 2015
Available online 7 February 2015

Keywords:
Strontium pyroniobate
Hydrothermal method
Nano materials
PXRD
TEM

ABSTRACT

$Sr_2Nb_2O_7$ nano-powders were synthesized via a hydrothermal reaction in a NaOH solution at 120 °C for 48 h followed by calcination at 400 °C for 3 h using $Sr(NO_3)_2$ and Nb_2O_5 in the nonstoichiometric 1:2 Sr:Nb molar ratio as raw materials. The synthesized materials were characterized by powder X-ray diffraction (PXRD) technique and Fourier transform infrared (FTIR) spectroscopy. To investigate the effect of concentration of the basic solutions on the morphology of the obtained materials, the morphologies of the synthesized materials were studied by field emission scanning electron microscopy (FESEM) technique. As shown by the FESEM measurements, the morphology of $Sr_2Nb_2O_7$ particles changed from mono-shaped flower and rod like structures to two kind flower structures by the NaOH concentration increase from 2 to 4 M. TEM images verified the nanometer size particle formation. Ultraviolet–visible spectra analysis showed that the nanostructured $Sr_2Nb_2O_7$ powder possessed strong light absorption in the ultraviolet light region.

1. Introduction

Strontium pyroniobate $Sr_2Nb_2O_7$ (SN) is a perovskite layer structure (PLS) compound. This compound is a ferroelectric material and has found several applications as a nonvolatile ferroelectric memory [1], optical waveguides [2] and a variety of other applications [3,4]. Photo catalytic water splitting reaction has also been studied extensively using this material as photo catalyst under ultraviolet (UV) irradiation [5–9]. Therefore, $Sr_2Nb_2O_7$ has attracted considerable attention due to its high potential as a novel photocatalyst for hydrogen production from water [10–12]. Also, textured $Sr_2Nb_2O_7$ is a promising candidate material for high-temperature piezoelectric sensors in automobiles, thermal power plants, and nuclear power plants because it has a very high Curie temperature of 1342 °C [13]. Several improved methods have been reported for the synthesis of $Sr_2Nb_2O_7$, including hydrothermal method at 240 °C for 48 h [12], sol–gel [14], PC molten salt route [13], sol–gel electrophoresis [15], solid state [16] and hydrothermal method at 200 °C for 24 h [17]. At room temperature, the $Sr_2Nb_2O_7$ orthorhombic unit cell parameters are $a = 3.933$, $b = 26.726$, and $c = 5.683$ Å. The crystal also exhibits strong cleavage parallel to the b plane [3]. The crystal structure of $Sr_2Nb_2O_7$ consists of vertex sharing NbO_6 octahedral units that are separated by additional O atoms [18–21]. $Sr_2Nb_2O_7$ is a part of a series having a chemical composition of $Sr_nNb_nO_{3n+2}$ [22] where n is the number of NbO_6 octahedrons comprising the slab thickness. Only $n = 4$ and $n = 5$ members of the series have been observed so far [22–24]. By Cooling from above the Curie temperature, [25] $Sr_2Nb_2O_7$ undergoes the ferroelectric phase transition from space group Cmcm to $Cmc2_1$, which is commonly referred to as the normal orthorhombic phase. On further cooling to 215 °C, the compound changes to an incommensurate (IC) phase with space group $Cmc2_1$ [26,27]. In the present study, a hydrothermal route followed by a calcination process was explored successfully to synthesize the nanostructured $Sr_2Nb_2O_7$ powders using $Sr(NO_3)_2$, Nb_2O_5 and NaOH as raw materials. To the best of our knowledge, there is no report on the synthesis of nanostructured $Sr_2Nb_2O_7$ crystallites by the low temperature hydrothermal method. The effect of NaOH concentration on the final product morphology was investigated and the band gap energy of the as prepared $Sr_2Nb_2O_7$ samples was estimated from UV–Visible spectra. Indeed, the conventional methods, like BET [28] and BJH [29] models and cell parameters observation were also performed.

2. Experimental section

All chemicals were of analytical grade, obtained from commercial sources, and used without further purification. Phase identifications were performed on a powder X-ray diffractometer D5000 (Siemens AG, Munich, Germany) using Cu Kα radiation with the

* Corresponding author. Fax: +98 233 338 3195.
E-mail addresses: mbehzad@semnan.ac.ir, mahdibehzad@gmail.com (M. Behzad).

http://dx.doi.org/10.1016/j.apt.2015.01.016

deviation of ±0.02°. The morphology of the obtained materials was examined with a field emission scanning electron microscope (Hitachi FE-SEM model S-4160). The material sizes were measured on a Zeiss – EM10C – 80 kV microscope. FT-IR spectra were recorded on a Tensor 27 (Bruker Corporation, Germany) with the deviation of ±2 cm^{-1}. Absorption and photoluminescence spectra were recorded on an Analytik Jena Specord 40 (Analytik Jena AG Analytical Instrumentation, Jena, Germany) with the deviation of ±1 nm and a Perkin Elmer LF-5 spectrometer (Perkin Elmer Inc., Waltham, MA, USA) with the deviation of ±1 nm, respectively. The surface area and pore volume and average nanoparticle size were calculated using the Brunauer–Emmett–Teller (BET) equation. Pore size distributions, pore volume and pore surface area were calculated by the Barrett–Joyner–Halenda (BJH) method. BET surface areas were acquired on a Beckman Coulter SA3100 Surface Area Analyzer. Cell parameter refinement was reported by celref software version 3 (Laboratoire des Materiaux et du Génie Physique de l'Ecole Supérieure de Physique de Grenoble).

3. Synthesis of $Sr_2Nb_2O_7$ nano materials

In a typical synthetic experiment, 0.16 g (0.75 mmol) of $Sr(NO_3)_2$ (M_w = 211.62 $gmol^{-1}$) and 0.20 g (0.75 mmol) of Nb_2O_5 (M_w = 265.82 $gmol^{-1}$) were added to 50 mL of hot aqueous solutions of 2 or 4 M NaOH (samples 1 or 2) under magnetic stirring at 80 °C, respectively. The resulting solution was stirred for further 15 min. Then it was transferred to a 100-mL Teflon lined stainless steel autoclave. The autoclave was sealed and heated at 120 °C for 48 h. When the synthesis was finished, the sample was cooled to room temperature into autoclave by quenching in water. The prepared powder was washed with distilled water and dried at 110 °C for 20 min under normal atmospheric conditions and was then treated thermally at 400 °C for 3 h and was left to cool down to room temperature to result the target.

4. Results and discussion

The phase composition of the nanomaterials synthesized from the solutions at different NaOH concentrations were examined by powder X-ray diffraction technique. The PXRD patterns recorded from samples S_1 and S_2 formed at 2 and 4 M NaOH aqua solution, respectively, are shown in Fig. 1. It is obvious that the NaOH concentration is a key factor affected the phase composition. The measured patterns are in good agreement with those of corresponding pure nanomaterials [14,12,23,30–33]. Besides, the obtained stable phases are isostructural with $Sr_2Nb_2O_7$ (space group $Cmc2_1$) [12,33]. Also, the measured data are in agreement with the respective Joint Committee on Powder Diffraction Standards (JCPDS) card for $Sr_2Nb_2O_7$ (JCPDS 70-0114). The $Sr_2Nb_2O_7$ unit cell is quite large, with a = 3.933, b = 26.726, and c = 5.683 Å [33]. Compared to the nanomaterials of 2 M NaOH solution synthesized (S_1), there is a difference in the peaks appearance of some diffraction that correspond to $Sr_2Nb_2O_7$ diffraction lines. It can cause a difference in the morphology of the obtained materials. Also, the diffraction lines in the XRD patterns of the (S_2) has shifted to higher 2θ values and therefore to lower d values. For the most intensive diffraction line (1 1 0), a diffraction line shift of $\Delta 2\theta = 22.86°$ (S_2) − 22.77° (S_1) = 0.09° (Δd = 3.902 Å (S_1) − 3.888 Å (S_2) = 0.014 Å) is calculated via Bragg's law.

Table 1 shows the crystal sizes of the as-synthesized nanomaterials in different NaOH concentration calculated via Scherrer equation, using the peak at hkl (1 1 0) corresponded to $Sr_2Nb_2O_7$ phase; $t = \frac{k\lambda}{B_{1/2}\cos\theta}$. In this equation, t is the entire thickness of the crystalline sample, λ is the X-ray diffraction wavelength (0.154 nm), and k is the Scherrer constant (0.9), $B_{1/2}$ of FWHM is the full width

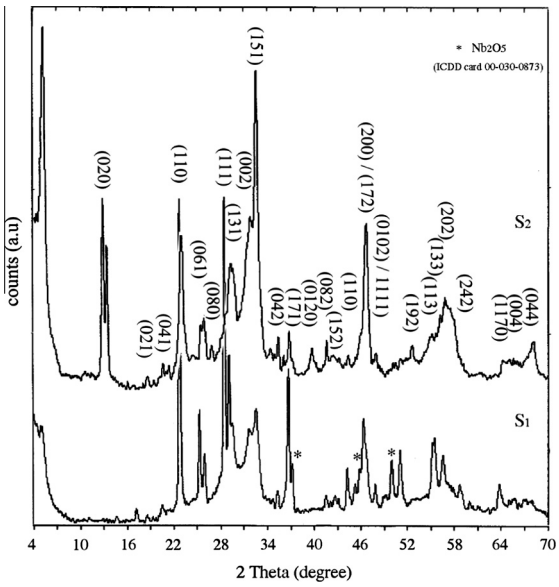

Fig. 1. PXRD patterns of the hydrothermally synthesized $Sr_2Nb_2O_7$ nanomaterials obtained after 48 h at 120 °C in 2 (S_1) and 4 M (S_2) NaOH solution.

at half its maximum intensity and θ is the half diffraction angle at which the peak is located. The data mentioned in Table 1 show that the calculated crystal size for S_2 is smaller than that of S_1. In other words, with increasing NaOH concentration, the crystal sizes become larger that is in agreement with TEM images. So, according to PXRD pattern, the calculated crystal size and interplanar spacing are in agreement with the grain size estimated from TEM images.

5. Microstructure analysis

Typical FESEM images recorded from sample 1 are shown in Fig. 2. From the FESEM images in Fig. 2a–c, with the magnification of 30,000×, 60,000× and 150,000×, respectively, it is obvious that the morphology of the obtained materials were in flower form, and the flowers were composed of the petals. At higher magnification to 200,000× in Fig. 2d, it is clear that the materials were composed of several petals crossed each other creating a flower form.

Fig. 3(a–d) with the magnifications of 60,000×, 80,000×, 100,000× and 60,000×, respectively, show FESEM images of sample S_2. At low magnification at 60,000×, it is indicated that the main product consists of 3-D architecture flower-type forms. Closer inspection of the higher magnification images shown in Fig. 3c and d revealed that the flowers were being composed of nanoflakes. There was another type flower structure which was different from the first type structure, as shown in Fig. 3e (10,0000×) and h (30,000×).

Fig. 4 shows the TEM images of the as-synthesized nano materials at 2 M NaOH solution at 120 °C. Two types of morphological structures are evident. One is rod like structures indexed with (a–c), and other is flower structures indexed with (e, f and h). As shown in Fig. 4(e, f and h), the petal thickness is 10 nm and the length is 61 nm. The rod structure length size is 130 nm and the width size is 18 nm. Fig. 4(d, g and i) shows the smallest particle sizes of the obtained materials. It shows that the particle size is 9 nm.

Fig. 5 shows the TEM images of the as-synthesized nano materials at 4 M NaOH solution at 120 °C. It shows that the obtained nanomaterials have homogenous flower structure. Fig. 5(a–d) and (g, h) shows that the petal thickness size is 12 nm and the length size is 110 nm.